BEHAVIOUR OF THE $AlCoCr_{0.5}NiY_{0.1}$ MULTI-PRINCIPAL ELEMENT ALLOY AT 1100°C

Olga Samoilova[1], Svetlana Pratskova[1,2], Arman Bilgenov[1],
Natalja Shaburova[1], Evgeny Trofimov[1], Sergey Lezhnev[3], Evgeniy Panin[4]

[1]South Ural State University, Chelyabinsk, Russia, samoilovaov@susu.ru (O.S.);
se_pratskova@mail.ru (S.P.); bilgenova@susu.ru (A.B.);
shaburovana@susu.ru (N.S.), trofimovea@susu.ru (E.T.).
[2]Chelyabinsk State University, Chelyabinsk, Russia
[3]Rudny Industrial University, Rudny, Kazakhstan, sergey_legnev@mail.ru (S.L.).
[4]Karaganda Industrial University, Temirtau, Kazakhstan, cooper802@mail.ru (E.P.).

Received 10 October 2025
Accepted 16 February 2026 *DOI: 10.59957/jctm.v61.i5.2026.16*

ABSTRACT

The microstructure and phase composition of cast $AlCoCr_{0.5}NiY_{0.1}$ multi-principal element alloy (MPEA) have been determined. High-temperature oxidation of the alloy under study was carried out at 1100°C for 100 h in an atmospheric atmosphere. The high resistance of this MPEA to high-temperature gas corrosion is shown, the parabolic oxidation rate constant was $k_p = 9.48 \times 10^{-13}$ g^2 cm^{-4} s^{-1}. It has been established that the introduction of yttrium is an effective way to increase the heat resistance of multi-principal element alloys.

Keywords: multi-principal element alloys, high-temperature oxidation resistance, reactive elements, yttrium, alloying, protective oxide film.

INTRODUCTION

The concept of "multi-principal element alloys" (MPEA) ("high-entropy alloys", HEA) It appeared in the early 2000s, and the idea proved to be a breakthrough in the field of new materials. The proposed concept suggested that the composition of the alloy is not based on one leading component but consists of elements in an equiatomic (or close to it) ratio [1]. However, it was later shown that these alloys can have a multivariate composition, where a number of components can vary in concentration from 5 to 30 atm. % [2]. This ensured the production of materials with unique properties. Thus, several $Al_xCoCrFeNi$ type alloys demonstrate excellent mechanical characteristics, tribological properties and high corrosion resistance in aggressive solutions [3 - 9]. And the increased concentrations of aluminium and chromium in the composition of such alloys have made them potential candidates for the role of heat-resistant alloys for high-temperature applications [10, 11].

Further studies have shown that doping MPEAs with a small amount of an additional introduced element can have a significant effect on their properties, including resistance to high-temperature oxidation [12, 13]. Yttrium is one of the so-called "reactive elements" and attracts the attention of researchers precisely for its potentially significant effect on the resistance of alloys to high-temperature gas corrosion [14]. Currently, there are several studies devoted to co-doped Y/Hf or Y/Hf/Ta high-entropy alloys, where the concentration of these highly active elements does not exceed hundredths of an at. % [15 - 19]. The results showed that wind turbines doped with a small number of reactive elements demonstrated excellent heat resistance, and the oxide film obtained on the surface (about 3 μm thick) consisted of a dense mass of crystallites (representing aluminium oxide Al_2O_3) and nanoparticles of Y/Hf oxides, which provided its high protective properties. Several works are devoted to the direct effect of yttrium on the properties of wind farms [20, 21]. The introduction of yttrium in the number of hundredths of an at. % in the eutectic high-entropy alloy $AlCoCrFeNi_{2.1}$ significantly improved the adhesion of the Al_2O_3 oxide film to the matrix material during high-temperature oxidation and also stabilized the eutectic microstructure during isothermal exposure at high temperatures.

An interesting area is the synthesis and study of the properties of $Al_xCoCrNiM_y$ type alloys (where M is an alloying additive). For example, the excellent corrosion resistance of Fe-free HEA AlCoCrNiNb is known [22]. At the same time, the alloy $Al_{20}Co_{25}Cr_{25}Ni_{25}Si_5$ has increased resistance to high-temperature gas corrosion [23]. It was found that a decrease in chromium concentration from the AlCoCrNi composition to the $AlCoCr_{0.5}Ni$ composition reduced the specific weight gain by half after 100 h isothermal exposure at 1100°C [24].

The purpose of this work is to study the heat resistance of the new Fe-free Y-doped $AlCoCr_{0.5}NiY_{0.1}$ MPEA. The study will evaluate the effect of the introduced yttrium on the resistance to high-temperature gas corrosion of the resulting alloy, as well as calculate the kinetic parameters of high-temperature oxidation and evaluate the protective characteristics of the oxide film formed after 100 h of isothermal exposure at 1100°C.

EXPERIMENTAL

The ingot of the composition $AlCoCr_{0.5}NiY_{0.1}$ was made by melting granules and powders of metals of high purity (> 99.9 wt. %) in the NABERTHERM VHT 8/22-GR vacuum furnace (Nabertherm GmbH, Lilienthal, Germany). The mixture of materials was loaded into an aluminum oxide crucible with a lid; melting was carried out at a temperature of 1670-1730°C. Three remelts were carried out to obtain a homogeneous microstructure.

The experiment on long-term oxidation was carried out in a muffle furnace Plavka-Pro PM-1 SmartKiln (Plavka.Pro Korolev, Russia) at 1100°C for 100 h in the air. The method of such an experiment was described in detail by us earlier in [25].

Microstructural analysis before and after oxidation was performed on a JEOL JSM7001F scanning electron microscope (SEM) (JEOL, Tokyo, Japan) equipped with an Oxford INCA X-max 80 energy dispersive X-ray spectroscopy (EMR) detector (Oxford Instruments, Abingdon, UK). X-ray diffraction (XFA) on a Rigaku Ultima IV X-ray diffractometer (Rigaku, Tokyo, Japan) using Cu-Ka radiation (λ = 0.15406 Å) was used to determine the phase composition of the metal and the oxide film.

RESULTS AND DISCUSSION

The cast alloy $AlCoCr_{0.5}NiY_{0.1}$ demonstrates a dendritic microstructure, where dendrites (D) are enriched in Al and Ni, and the dendritic interlayers (ID) contain elevated concentrations of Co and Cr (Fig. 1a, Table 1). Inclusions containing yttrium (Y) are arranged in groups (bright white dots), which are found throughout the entire area of the slot, both in dendrites and in the inter-dendritic space. The size of such inclusions does not exceed 10 μm, and for the most part they range from 1 to 3 μm.

According to the X-ray phase analysis data (Fig. 1b), the cast sample $AlCoCr_{0.5}NiY_{0.1}$ MPEA is characterized by the presence of two solid solutions with a face-centered cubic crystal lattice (HCC) and a volume-centered cubic crystal lattice (BCC). Earlier it was determined that the BCC solid solution is enriched in Al and Ni; the HCC solid solution in polybasic alloys contains higher concentrations of Co and Cr [26]. Thus, the dendrites in the $AlCoCr_{0.5}NiY_{0.1}$ MPEA microstructure can be attributed to the BCC solid solution, and the dendritic interlayers have the HCC structure. The yttrium on the diffractogram did not produce reflexes, apparently because the slot area occupied by it is less than 5 %, which is beyond the sensitivity of the equipment used.

Fig. 2 shows the results on the change in the specific weight gain of the alloy under study during a 100 h isothermal exposure at 1100°C. The maximum specific weight gain for $AlCoCr_{0.5}NiY_{0.1}$ MPEA was 0.493 mg cm^{-2}, which significantly exceeds the results of Jang et al., according to which, after exposure for 50 h at 1100°C, the maximum specific weight gain of the Inconel 617 industrial alloy was 1.8 mg cm^{-2} [27]. The values obtained by us can be compared with the data from Butler and Weaver, which indicate figures of 0.5 mg cm^{-2} and 1.1 mg cm^{-2} after 100 h isothermal exposure at 1050°C. for compositions $Al_{30}(NiCrCoFe)_{70}$ and $Al_{12}(NiCrCoFe)_{88}$, respectively [28].

The general formula for oxidation kinetic can be represented as Eq. (1) [29]:

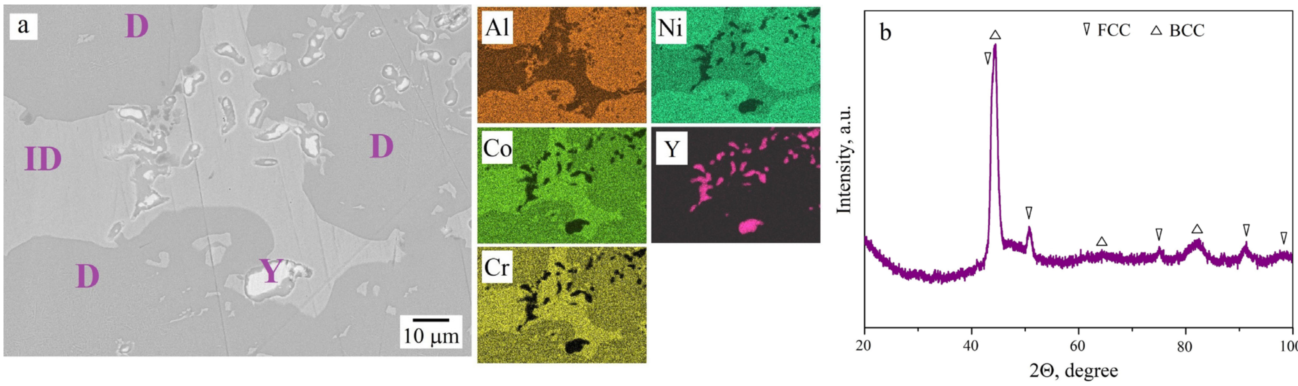

Fig. 1. Microstructure according to SEM (backscattered electrons) with corresponding EDS mapping (a) and diffraction pattern (b) of the as-cast $AlCoCr_{0.5}NiY_{0.1}$ MPEA.

Table 1. Chemical composition (according to EDS, at. %). Av - average composition; D - dendrite; ID - interdendritic space; Y - Y-containing precipitation; OF - oxide film (after isothermal holding).

		Al	Co	Cr	Ni	Y	O
$AlCoCr_{0.5}NiY_{0.1}$	Av	27.77	27.35	14.39	27.53	2.96	-
	D	31.54	24.92	7.04	36.50	-	-
	ID	13.65	38.05	23.03	25.27	-	-
	Y	14.92	2.34	0.86	1.99	79.89	-
	OF	39.47	0.86	0.92	0.68	0.05	58.02

$$\frac{\Delta m}{A} = k\tau^n , \quad (1)$$

in which k and n are the simplify oxidation coefficient and dimensionless oxidation exponent respectively (time is given in h). The n value can represent the different oxidation behaviours (n = 1, 0.5 and 0.33 correspond to the linear, parabolic and cubic oxidation behaviours, respectively). The calculation results are presented in Fig. 2.

Even though the oxidation was closer to the cubic law than the parabolic one, we performed calculations for the parabolic oxidation rate constant for the convenience of comparing the data we obtained with the literature, since most of the calculations presented in the literature were performed for the parabolic nature of oxidation.

Specific weight change (W) in parabolic law can be related to time as Eq. (2):

$$\left(\frac{\Delta m}{A}\right)^2 = k_p\tau , \quad (2)$$

where Δm is mass change (g), A is surface area (cm^2),

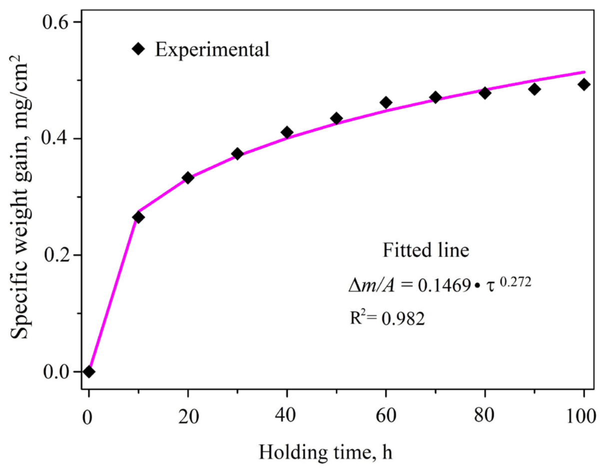

Fig. 2. Kinetic curve of oxidation at 1100°C for $AlCoCr_{0.5}NiY_{0.1}$ MPEA.

k_p is parabolic oxidation rate constant (g^2 cm^{-4} s^{-1}), and τ is the holding time (s).

The k_p calculation results for $AlCoCr_{0.5}NiY_{0.1}$ MPEA in comparison with the literature data are shown in the Table. 2. As it can be seen, the rate of oxidation of $AlCoCr_{0.5}NiY_{0.1}$ MPEA is comparable to the rate of oxidation of Y-containing wind turbines and much lower compared to wind turbine compositions that do not contain yttrium [24, 28, 30].

The compliance of the oxidation process with the cubic law means that the formed oxide film on the surface of $AlCoCr_{0.5}NiY_{0.1}$ MPEA has excellent protective properties. This is consistent with the results of the study of its surface morphology (Fig. 3). It can be noted that the formed oxide layer is homogeneous, has no defects and consists of a dense mass of needle-like crystallites with a thickness of less than 1 μm. In terms of chemical composition, it is mainly represented by aluminium and oxygen (see Table. 1), the concentration of Co, Cr and Ni does not exceed 1 atm. %, the layer also contains practically no yttrium in its composition.

The study of the transverse section of the alloy sample after the experiment confirms the uniformity of the chemical composition of the surface oxide layer (Fig. 4). In this case, the main elements composing this layer are aluminium and oxygen, which are evenly distributed throughout its thickness. It is possible to note the excellent adhesion of the film to the matrix material, there are no defects on the border, the film adheres tightly to the metal. The thickness of the oxide layer is

Table 2. Parabolic oxidation rate constant (k_p, g^2 cm^{-4} s^{-1}) of $AlCoCr_{0.5}NiY_{0.1}$ MPEA compared to other works.

Alloy	t, °C	k_p	Alloy	t, °C	k_p
$AlCoCr_{0.5}NiY_{0.1}$	1100	9.48×10^{-13}	AlCoCrFeNi [24]	1100	89×10^{-13}
AlCoCrFeNiY/Hf [15]	1100	1.9×10^{-13}	AlCoCrNi [24]	1100	200×10^{-13}
AlCoCrFeNiY/Ta [19]	1100	15.72×10^{-13}	$AlCoCr_{0.5}Ni$ [24]	1100	40×10^{-13}
AlCoCrFeNiY/Ta/Hf [19]	1100	6.75×10^{-13}	$Al_{30}(CoCrFeNi)_{70}$ [28]	1050	19×10^{-13}
$AlCoCrFeNi_{2.1}Y$ [20]	1100	10×10^{-13}	$AlCoCr_{0.5}NiNb_{0.2}$ [30]	1100	148.83×10^{-13}

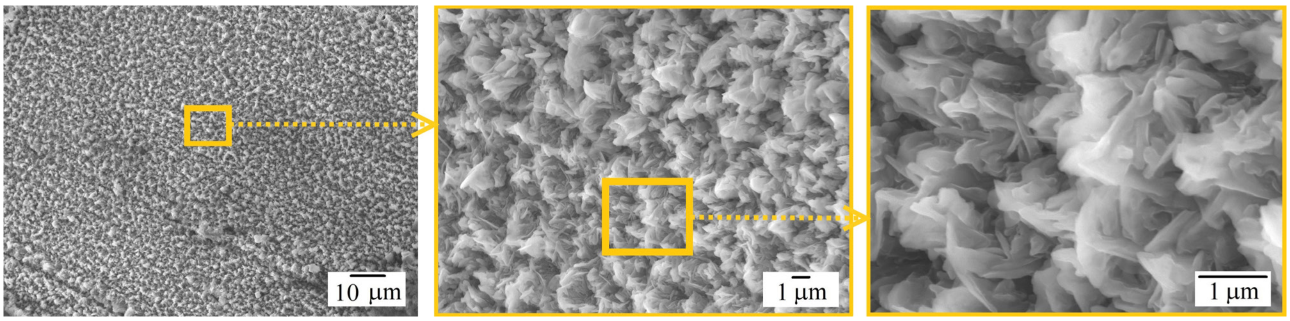

Fig. 3. Morphology of the surface of the oxide film formed after 100 h isothermal exposure at 1100°C at $AlCoCr_{0.5}NiY_{0.1}$ MPEA.

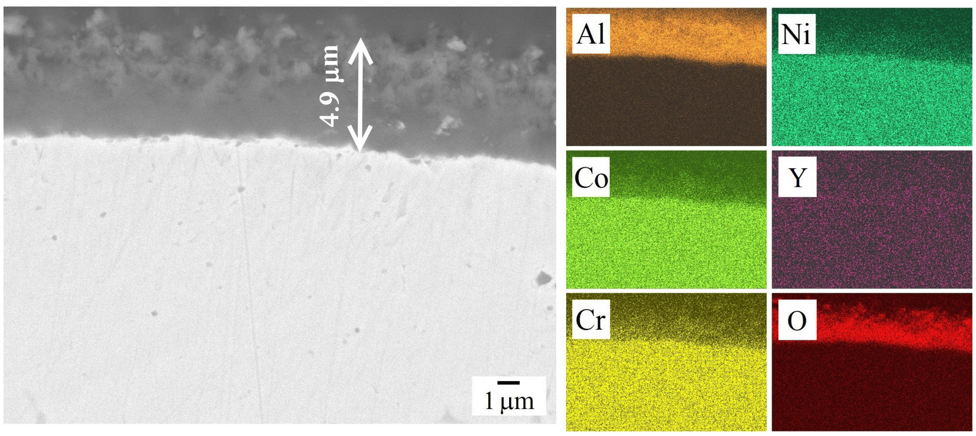

Fig. 4. Transverse section of an $AlCoCr_{0.5}NiY_{0.1}$ alloy sample after 100 h isothermal exposure at 1100°C.

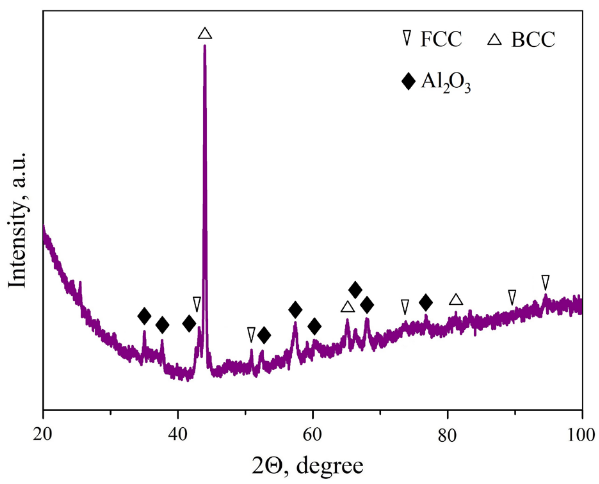

Fig. 5. Diffractogram of the surface of an $AlCoCr_{0.5}NiY_{0.1}$ alloy sample after 100 h isothermal exposure at 1100°C.

about 5 ± 1 μm (according to at least 20 measurements) and has practically no significant size differences.

The results of the X-ray phase analysis of the sample surface after the experiment (Fig. 5) are consistent with the EDS data: in addition to peaks from the matrix material, the diffractogram shows reflections only from aluminium oxide Al_2O_3.

Thus, yttrium does not directly affect, but indirectly, the resistance to high-temperature oxidation, provoking the formation of a dense protective film of aluminium oxide. This corresponds to its characteristics as a "reactive element" and a catalyst for accelerating the diffusion of aluminium ions. A similar effect from the introduction of yttrium is noted in [15, 20, 21]. At the same time, resistance to high-temperature oxidation is more likely to be affected by hundredths or thousandths of a percent of yttrium dissolved in solid solutions than by its particles released by a separate phase.

CONCLUSIONS

Based on the results of the study, it can be concluded that yttrium is an element, the alloying of which can increase the resistance to high-temperature oxidation of multi-principal element alloys. The introduction of yttrium provokes the formation of a dense protective film consisting of aluminum oxide on the surface of the alloy during isothermal exposure at 1100°C. At the same time, the adhesion of the film to the matrix material is excellent, and the film thickness does not exceed 6 μm around the entire perimeter of the test sample. However, this effect of yttrium is more likely due to micro-concentrations in solid solutions rather than to the release of its individual particles. Therefore, in further studies, the yttrium content in the alloy can be reduced to the level of microalloying (hundredths of a percent), which will increase the economic efficiency of its use.

Acknowledgements

The study was supported by the Russian Science Foundation and the Government of the Chelyabinsk Region, project No. 25-23-20049. https://rscf.ru/project/25-23-20049/

Authors' contributions

O.S.: methodology, investigation, writing - original draft; S.P.: investigation, funding acquisition, project administration; A.B.: conceptualization, methodology, investigation; N.S.: visualization, investigation; E.T.: validation, data curation; S.L.: software, writing - review & editing; E.P.: formal analysis, resources.

REFERENCES

1. B. Cantor, I.T.H. Chang, P. Knight, A.J.B. Vincent, Microstructural development in equiatomic multicomponent alloys, Mater. Sci. Eng. A., 2004, 375-377, 213-218. https://doi.org/10.1016/j.msea.2003.10.257.
2. E.P. George, D. Raabe, R.O. Ritchie, High-entropy alloys, Nat. Rev. Mater., 2019, 4, 515-534. https://doi.org/10.1038/s41578-019-0121-4.
3. Z. Li, K.G. Pradeep, Y. Deng, D. Raabe, C.C. Tasan, Metastable high-entropy dual-phase alloys overcome the strength-ductility trade-off, Nature, 2016, 534, 227-230. https://doi.org/10.1038/nature17981.
4. E.P. George, W.A. Curtin, C.C. Tasan, High entropy alloys: A focused review of mechanical properties and deformation mechanisms, Acta Mater., 2020, 188, 435-474. https://doi.org/10.1016/j.actamat.2019.12.015.
5. S. Jain, R. Jain, V. Kumar, S. Samal, J. Lee, Design strategies and mechanical behaviour of high-strength eutectic high-entropy alloys: a comprehensive review, Journal of Alloys and Compounds, 2025, 1022, 180000. https://doi.org/10.1016/j.jallcom.2025.180000.
6. A.K. Kasar, K. Scalaro, P.L. Menezes, Tribological properties of high-entropy alloys under dry conditions for a wide temperature range - A review, Materials, 2021, 14, 5814. https://doi.org/10.3390/ma14195814.
7. A. Ostovari Moghaddam, M.N. Samodurova, K. Pashkeev, M. Doubenskaia, A. Sova, E.A. Trofimov, A novel intermediate temperature self-lubricating $CoCrCu_{1-x}FeNi_x$ high entropy alloy fabricated by direct laser cladding, Tribology International, 2021, 156, 106857. https://doi.org/10.1016/j.triboint.2021.106857.
8. Y. Shi, B. Yang, P.K. Liaw, Corrosion-resistant high-entropy alloys: A review, Metals, 2017. 7, 43,.https://doi.org/10.3390/met7020043.
9. O. Samoilova, S. Pratskova, N. Shaburova, A. Ostovari Moghaddam, E. Trofimov, Corrosion resistance of $CoCrFeNiMo_x$ (x = 0.1, 0.3, 0.5) high-entropy alloys in aggressive aqueous solutions containing Cl^- or SO_4^{2-} ions, Journal of Materials Engineering and Performance, 2025, 34, 25554-25564. https://doi.org/10.1007/s11665-025-11090-z.
10. P. Kumar, T.-N. Lam, P.K. Tripathi, S.S. Singh, P.K. Liaw, E.-W. Huang, Recent progress in oxidation behavior of high-entropy alloys: A review, APL Mater, 2022, 10, 120701. https://doi.org/10.1063/5.0116605.
11. H. Shahbazi, H. Vakilifard, R.B. Nair, A.C. Liberati, R.S. Lima, P. Stoyanov, C. Moreau, High entropy alloy bond coats for thermal barrier coatings: A review, J. Therm. Spray. Tech., 2024, 33, 430-446. https://doi.org/10.1007/s11666-023-01701-3.
12. Y. Yu, N. Xu, S. Zhu, Z. Qiao, J. Zhang, J. Yang, W. Liu, A novel Cu-doped high entropy alloy with excellent comprehensive performances for marine application, Journal of Materials Science and Technology, 2021, 69, 48-59. https://doi.org/10.1016/j.jmst.2020.08.016.
13. S. Brito-Garcia, J. Mirza-Rosca, V. Geanta, I. Voiculescu, Mechanical and Corrosion Behavior of Zr-Doped High-Entropy Alloy from CoCrFeMoNi System, Materials, 2023, 16, 1832. https://doi.org/10.3390/ma16051832.
14. D.P. Whittle, J. Stringer, Improvements in High Temperature Oxidation Resistance by Additions of Reactive Elements or Oxide Dispersions, Phil. Trans. R. Soc. Lond. A, 1980, 295, 309-329. https://doi.org/10.1098/rsta.1980.0124.
15. J. Lu, Y. Chen, H. Zhang, N. Ni, L. Li, L. He, R. Mu, X. Zhao, F. Guo, Y/Hf-doped AlCoCrFeNi high-entropy alloy with ultra oxidation and spallation resistance, Corros. Sci., 2020, 166, 108426. https://doi.org/10.1016/j.corsci.2019.108426.
16. J. Lu, Y. Chen, H. Zhang, L. Li, L. Fu, X. Zhao, F. Guo, P. Xiao, Effect of Al content on the oxidation behavior of Y/Hf-doped AlCoCrFeNi high-entropy alloy, Corros. Sci., 2020, 170, 108691. https://doi.org/10.1016/j.corsci.2020.108691.
17. J. Lu, Y. Chen, H. Zhang, L. He, R. Mu, Z. Shen, X. Zhao, F. Guo, Y/Hf-doped $Al_{0.7}CoCrFeNi$ high-entropy alloy with ultra oxidation and spallation resistance at 1200°C, Corros. Sci., 2020, 174, 108803. https://doi.org/10.1016/j.corsci.2020.108803.
18. J. Lu, H. Zhang, L. Li, A. Huang, X. Liu, Y. Chen, X. Zhang, F. Guo, X. Zhao, Y-Hf co-doped

$Al_{1.1}CoCr_{0.8}FeNi$ high-entropy alloy with excellent oxidation resistance and nanostructure stability at 1200°C, Scripta Materialia, 2021, 203, 114105. https://doi.org/10.1016/j.scriptamat.2021.114105.

19. J. Hu, C. Gu, J. Li, C. Li, J. Feng, Y. Jiang, Microstructure and oxidation behavior of the Y/Ta/Hf co-doped AlCoCrFeNi high-entropy alloys in air at 1100°C, Corros. Sci., 2023, 212, 110930. https://doi.org/10.1016/j.corsci.2022.110930.
20. J. Lu, H. Zhang, Y. Chen, L. Ling, X. Liu, W. Xiao, N. Ni, X. Zhao, F. Guo, P. Xiao, Y-doped $AlCoCrFeNi_{2.1}$ eutectic high-entropy alloy with excellent oxidation resistance and structure stability at 1000 °C and 1100°C, Corros. Sci., 2021, 180, 109191. https://doi.org/10.1016/j.corsci.2020.109191.
21. X. Sun, X. Li, S. Guo, L. Zhu, J. Teng, L. Jiang, J. Moverare, X.-H. Li, R.L. Peng, The impact of Al/Cr ratio on the oxidation kinetics of Y-doped AlCoCrFeNi high-entropy alloys at 1100°C, Intermetallics, 2025, 176, 108582. https://doi.org/10.1016/j.intermet.2024.108582.
22. B. Pan, X. Xu, J. Yang, H. Zhan, L. Feng, Q. Long, Q. Yao, J. Deng, L. Cheng, Z. Lu, H. Zhou, Effect of Nb, Ti, and V on wear resistance and electrochemical corrosion resistance of $AlCoCrNiM_x$ (M=Nb, Ti, V) high-entropy alloys, Materials Today Communications, 2024, 39, 109314. https://doi.org/10.1016/j.mtcomm.2024.109314.
23. R. Gawel, Ł. Rogal, Z. Grzesik, Behaviour of Al, Co, Cr, Ni-based high entropy alloys under high-temperature thermal shock oxidising conditions, Corros. Sci., 2022, 198, 110116. https://doi.org/10.1016/j.corsci.2022.110116.
24. A. Anupam, A.S.M. Ang, K. Guruvidyathri, M. Abbas, D. Sivaprahasam, P. Munroe, C.C. Berndt, B.S. Murty, R.S. Kottada, Evaluating the influence of microstructural attributes: Fraction, composition, size and spatial distribution of phases on the oxidation behaviour of high-entropy alloys, Corros. Sci., 2021, 184, 109381. https://doi.org/10.1016/j.corsci.2021.109381.
25. O. Samoilova, I. Suleymanova, N. Shaburova, A. Ostovari Moghaddam, E. Trofimov, The behavior of $Al_{0.5}CoCrFeNiCuPt_{0.3}$ high-entropy alloy during high-temperature oxidation, High Temperature Corrosion of Materials, 2024, 101, 4, 811-825. https://doi.org/10.1007/s11085-024-10248-9.
26. O. Samoilova, M. Sudarikov, N. Shaburova, A. Ostovari Moghaddam, E. Trofimov, High temperature oxidation resistance of $AlCoCrFeNiCu_{0.25}W_{0.1}$ high-entropy alloy, MRS Advances, 2025 (article in press). https://doi.org/10.1557/s43580-025-01334-4.
27. C. Jang, D. Lee, D. Kim, Oxidation behaviour of an Alloy 617 in very high-temperature air and helium environments, International Journal of Pressure Vessels and Piping, 2008, 85, 6, 368-377. https://doi.org/10.1016/j.ijpvp.2007.11.010.
28. T.M. Butler, M.L. Weaver, Oxidation behavior of arc melted AlCoCrFeNi multi-component high-entropy alloys, Journal of Alloys and Compounds, 2016, 674, 229-244. https://doi.org/10.1016/j.jallcom.2016.02.257.
29. T. Onishi, S. Nakakubo, M. Takeda, Calculations of internal oxidation rate equations and boundary conditions between internal and external oxidation in silicon containing steels, Mater. Trans., 2010, 51,3, 482-487. https://doi.org/10.2320/matertrans.M2009256.
30. O. Samoilova, S. Pratskova, N. Shaburova, A. Ostovari Moghaddam, E. Trofimov, High-Temperature Oxidation Resistance of Fe-Free $AlCoCrNiNb_{0.2}$ and $AlCoCr_{0.5}NiNb_{0.2}$ High-Entropy Alloys, Materials, 2025, 18, 3701. https://doi.org/10.3390/ma18153701.